Simultaneous imaging of cell and mitochondrial membrane potentials

Daniel L. Farkas, Mei-de Wei, Peter Febbroriello, John H. Carson, and Leslie M. Loew
Departments of Biochemistry and Physiology, University of Connecticut Health Center, Farmington, Connecticut 06032

ABSTRACT The distribution of charged membrane-permeable molecular probes between intracellular organelles, the cytoplasm, and the outside medium is governed by the relative membrane electrical potentials of these regions through coupled equilibria described by the Nernst equation. A series of highly fluorescent cationic dyes of low membrane binding and toxicity (Ehrenberg, B., V. Montana, M.-D. Wei, J. P. Wuskell, and L. M. Loew, 1988. *Biophys. J.* 53:785–794) allows the monitoring of these equilibria through digital imaging video microscopy. We employ this combination of technologies to assess, simultaneously, the membrane potentials of cells and of their organelles in situ. We describe the methodology and optimal conditions for such measurements, and apply the technique to concomitantly follow, with good time resolution, the mitochondrial and plasma membrane potentials in several cultured cell lines. The time course of variations induced by chemical agents (ionophores, uncouplers, electron transport, and energy transfer inhibitors) in either or both these potentials is easily quantitated, and in accordance with mechanistic expectations. The methodology should therefore be applicable to the study of more subtle and specific, biologically induced potential changes in cells.

INTRODUCTION

Most cells maintain a significant electrical potential difference across their membranes at the expense of metabolic energy. The involvement and importance of these potentials in a variety of cellular functions (development, signaling, movement, regulation, energy balance, etc.) has long been recognized. Correlations have not always been easy to establish however, due to difficulties arising from the complexity of the systems under scrutiny and the limitations of the methods used for assessing potentials. Intracellular organelles such as mitochondria possess function-related membrane potentials far exceeding that of the plasma membrane, but their evaluation has proved even more difficult, especially in situ. It is clear that simultaneous measurement of both membrane potentials could provide important information on the role of electrical events in cell function.

The usefulness of fluorescent dyes as membrane potential indicators could hardly be overstated, and numerous reviews have catalogued progress in the development of this method (e.g., Cohen and Salzberg, 1978; Waggoner, 1979, 1985; Freedman and Laris, 1981; Loew, 1988). Especially useful for this work are two very recent reviews which focus on optical probes of membrane potential in nonexcitable cells (Freedman and Laris, 1988) and subcellular organelles (Smith, 1988). The most widely used indicators are the so-called redistribuiton dyes, primarily by virtue of their large response to potential changes. The mechanisms involved often require specific membrane binding or dye aggregation, thus narrowing the range of applications and acceptable experimental conditions and increasing the stringency of calibration requirements. This also restricts the ability of redistribution probes to simultaneously monitor potential changes in cells and intracellular organelles; indeed, the very existence of one of these potentials can be a hinderance in the measurement of the other, in certain experimental approaches (Korchak et al., 1982; Ritchie, 1984).

This laboratory recently developed a series of highly fluorescent cationic redistribution dyes which have low membrane affinities and do not aggregate (Ehrenberg et al., 1988). Their distribution across the plasma membrane is governed primarily by the Nernst equation:

$$V = -(RT/ZF) \ln (c_i/c_o), \quad (1)$$

where V is the membrane electrical potential (negative inside), Z is the charge of the permeable ion, F is Faraday's constant, R is the ideal gas constant, T is the absolute temperature, and c_i and c_o the inside and outside probe concentrations. Because the conditions of low self association and low background binding to cellular components are met, the total fluorescence of cell suspensions containing these dyes is not sensitive to changes in membrane potential; however, after correction for a small amount of nonpotential dependent binding, the ratio of the fluorescence intensity inside to that outside any particular cell equals the concentration ratio appearing in Eq. 1, thus allowing determination of the membrane potential at equilibrium.

0006-3495/89/12/1053/17 $2.00

For intracellular organelles such as mitochondria, possessing their own membrane potential, the cytosol constitutes the outer medium from where the dye gets concentrated into the intramitochondrial volume, as described by a relation analogous to Eq. 1:

$$V_m = -(RT/ZF) \ln (c_m/c_i), \quad (2)$$

where V_m is the mitochondrial membrane potential, c_m and c_i are the dye concentrations inside the mitochondria and in the cell cytoplasm, respectively, and all other symbols are the same as in Eq. 1.

Eqs. 1 and 2 describe coupled equilibria, and by combining them one can underscore the fact that the concentration the dye reaches in the mitochondria depends not only on the mitochondrial but the plasma membrane potential as well:

$$c_m = c_o \exp [-(V + V_m)ZF/RT]. \quad (3)$$

We report here the simultaneous monitoring of intramitochondrial and intracellular fluorescence levels of the dyes successfully used previously (Ehrenberg et al., 1988). This is possible with digital video imaging microscopy, which permits us to record the spatial distribution of fluorescence intensity with good temporal resolution. Thus, we were able to follow the changes in either potential induced by a variety of chemical agents of known mechanism of action. These agents produced distinct and characteristic patterns of fluorescence changes depending on whether the mitochondria, plasma membrane, or both were affected. In addition, we present data obtained via confocal laser scanning microscopy which shows that it is possible to image the membrane potential of a single mitochondrion within a cell.

MATERIALS AND METHODS

Dyes and other chemicals

Tetramethyl rhodamine methyl ester (TMRM)[1] and tetramethyl rhodamine ethyl ester (TMRE) were prepared as previously described (Ehrenberg et al., 1988). For comparison, rhodamine-6G and rhodamine 123 (laser grade Eastman Kodak, Co., Rochester, NY) were also used in certain experiments. Dyes were added to the media from freshly prepared ethanol stock solutions, and ethanol concentrations in the media were never >0.1%.

All other chemicals were of the highest degree of purity commercially available. Antimycin A, ATP, gramicidin, monensin, nigericin, oligomycin, rotenone, and sodium tetraphenylborate were from Sigma Chemical Co., St. Louis, MO; trypan blue and valinomycin from Aldrich Chemical Co., Milwaukee, WI. They were all added to the media from fresh stock solutions.

[1] *Abbreviations used in this paper:* AOI, area of interest; EBSS, Earle's balanced salt solution; KEBSS, EBSS with Na^+ replaced with K^+; SIT, silicon intensified target; TMRE, tetramethylrhodamine ethyl ester; TMRM, tetramethylrhodamine methyl ester; TPB, tetraphenylborate.

Cells

HeLa cells were grown in Dulbecco's modified Eagle's essential medium (Gibco, Grand Island, NY), usually on 22 × 30-mm coverslips to facilitate subsequent microscopic observation. Before use, they were washed several times with Earle's balanced salt solution (EBSS, Gibco), having high NaCl concentrations (116.4 mM) and low KCl (5.4 mM). After wiping their margins and reverse sides dry, the coverslips were placed with the cells facing the interior of the observation chamber (see below) filled with EBSS and the dye of choice in the desired concentration.

Macrophage cells of the mouse J774.2 line were grown similarly on coverslips in Dulbecco's modified Eagle's minimal essential medium, as described previously (Ehrenberg et al., 1988). Washing and exposure to the dyes were by either EBSS or a buffer containing (in millimolar) 118 NaCl, 5 KCl, 1.3 $CaCl_2$, 0.8 $MgSO_4$, 9 Na_2CO_3, 5.5 glucose, and 20 Hepes, pH 7.4.

Melanoma cells (of the Cloudman S-91 mouse line, subclone M-3, CCL 53.1; American Type Culture Collection, Rockville, MD) were a kind gift from Dr. Susan Preston. They were also grown on 22 × 30-mm coverslips, in RPMI medium supplemented with 10% fetal bovine serum (Gibco).

For testing the influence of ion concentrations on the events monitored, and in particular to potentiate the action of ion-selective ionophores, we used a modified EBSS buffer containing no NaCl, 170 mM KCl and 13.1 mM $NaHCO_3$ instead of the usual 26.2 mM (denoted KEBSS in the following). For the J774.2 cells we also used a buffer in which 118 mM KCl simply replaced the same concentration of NaCl (hereafter, K buffer).

Assays of cell viability

The possible toxicity of the dyes toward the cell lines used was tested by trypan blue exclusion (Paul, 1970). Cells, either untreated or exposed to TMRM or TMRE in concentrations from 0.1 to 1 μM for various times, were washed with EBSS containing 0.4% trypan blue, and stained cells were counted in a hemocytometer. The influence of added ionophores and inhibitors on cell viability was also similarly tested.

Metabolic effects of the dyes were estimated by assessing intracellular ATP content through the luciferin–luciferase coupled enzymatic assay (Leach and Webster, 1986). Cells were grown as described above (but in petri dishes), stream-detached, resuspended at 10^7/ml, and incubated at 37°C in centrifuge tubes with various concentrations of TMRM and TMRE for times up to 200 min, significantly longer than the duration of any of the experiments reported here. After incubation, cells were pelleted and the medium removed. The pellet was treated at 0°C for 5 min with 1 ml of trichloracetic acid, and the mixture brought to pH 7.8 by addition of Tris crystals. After centrifugation, the supernatant was placed in a 0.5-cm pathlength quartz cuvette and 200 μl of the luciferin–luciferase assay mixture (Sigma Chemical Co.) were added. Luminescence emitted at 550 ± 10 nm was determined and recorded with a spectrofluorometer (model MPF 44B, Perkin-Elmer Corp., Norwalk, CT) and calibrated by addition of known amounts of ATP (Sigma Chemical Co.).

The preservation of cell structural integrity upon long exposure to dyes was monitored by light-microscopic observation (phase-contrast), whereas that of mitochondria was assessed by electron microscopy. Cell monolayers on glass coverslips, either untreated or exposed to 0.1 or 0.5 μM TMRE for 1 h at 37°C were fixed in 2% glutaraldehyde and processed as described by Preston et al. (1987) for thin-section electron microscopy.

Chamber design and temperature control

The chamber used in most of the experiments (similar to that described by Berg and Block, 1984) was machined out of clear plexiglass, glued onto a standard size microscope glass slide, forming in the center of it a shallow (≈1 mm) enclosure bordered on top by the coverslip on which the cells were grown (held in position by silicone grease or paraffin). Channels to two large open wells on the sides permitted liquid exchange without air bubble formation. By adding to one well while aspirating the other, we could switch the medium bathing the cells in a few seconds. Optically, this arrangement allowed microscopic observation in epifluorescence and phase contrast, either independently or simultaneously.

Temperature control of the samples throughout the experiments was achieved by either use of a thermostated air curtain (Sage Instruments, Boston, MA), or a temperature-controlled microscope stage.

Quantitative fluorescence microscopy

An Ortholux II binocular research microscope (E. Leitz, Inc., Rockleigh, NJ) equipped for phase contrast–transmitted light and epi-illumination–excited fluorescence measurements was slightly modified by inclusion in the respective light paths of two electronic Uniblitz shutters (Vincent Associates, Rochester, NY), allowing (under computer control) the choice of exposure timing to minimize bleaching and to facilitate automated data acquisition. The light source was a 100-W tungsten lamp routinely operated at about half-power. The objectives used (NPL Fluotar 40× and 100× oil immersion) had very high numerical apertures (1.30). For fluorescence studies, the Leitz M2 filter module with dichroic beam splitter and additional blocking filters was used, affording narrow green band (centered on 546 nm) excitation and detection above 590 nm, as required for rhodamine dyes.

The fluorescence and/or phase contrast image of the specimen was recorded at the video rate of 30 frames/s by a silicon intensified target (SIT) camera (model SIT 66, Dage-MTI, Inc., Michigan City, IN) and relayed to a monitor, a VCR (Panasonic AG-6300), a time-date generator (Panasonic WJ-810), and an image processing system (Recognition Technology, Inc., Westborough, MA).

Within the image processor, controlled by an 80286-based microcomputer (Standard 286/10 from PC Source, Austin, TX), the image was digitized with 512 × 512 pixel spatial and eight-bit intensity resolution via a frame grabber and stored in one of three frame buffers or directly onto the computer's hard disk (capacity, 70 MB with streaming tape back-up). Simple image manipulations such as spatial and temporal averaging (at the video rate), display of difference images, pseudocolor representations and histograms of intensities, etc., are made possible by the 16-bit arithmetic/logic unit of the processor. Software to integrate the operation of the microscope, shutters, image processor, and hard disk storage was custom written in "C" (Kochan, 1983), also allowing the use of the controlling microcomputer (80286 processor + 80287 math coprocessor) cpu for complex operations such as floating point image ratioing. A home-built i/o card in one of the computer's expansion slots, with hard-wire connections to the peripheral devices (shutters, VCR), allowed complete interactive software control of the sequence of events. Data analysis was performed with a software package built around the subroutine library supplied with the image processor. Over the range of light intensities used in our studies, the response of the SIT camera was quite linear, as verified by use of calibrated neutral density filters that attenuated the intensities of either the transmitted light (as in Barrows et al., 1984), the fluorescence excitation beam (see Fig. 1), or the fluorescence emitted, respectively.

Cells on the coverslip were bathed in the appropriate buffer within the chamber on the microscope stage, at a preselected temperature. The medium was then replaced by the same buffer, to which typically 0.1 μM (see Results) TMRE was added, and the equilibration of dye with the cell was monitored. A group of cells (usually two to six, in the same field but not in contact) was chosen, and a rectangular area of interest (AOI) encompassing them defined via the image processor's cursor controls. Successive images of this AOI were then stored on the hard disk, at intervals of our choice (typically 0.5–5 min), by averaging a preset number of frames (8–32) to provide enhanced signal/noise ratios. The excitation shutter was programmed to open three frame periods (90 ms) before image acquisition started (to allow for the camera's response time) and close immediately after. After full dye equilibration, changes in the membrane potentials could be induced by rapidly flushing the chamber with the medium containing the perturbant (maintaining the same dye concentration). The ensuing changes were then monitored in the same area of interest. After subtraction of a background image (obtained in the absence of light) and ratioing with the extracellular fluorescence (obtained by imaging an AOI of the same size but devoid of cells), each of the images in the sequence could be analyzed and displayed in a collage (as those in Figs. 5–10). Differential evaluation of the intensity changes in the mitochondrial and cytoplasmic areas was facilitated by taking advantage of their significantly different and relatively narrow intensity ranges. By use of the image processor's capabilities, binary templates could be created within the cells, identifying the respective regions, and the changes in fluorescence intensity upon perturbation could be separately analyzed (see Results).

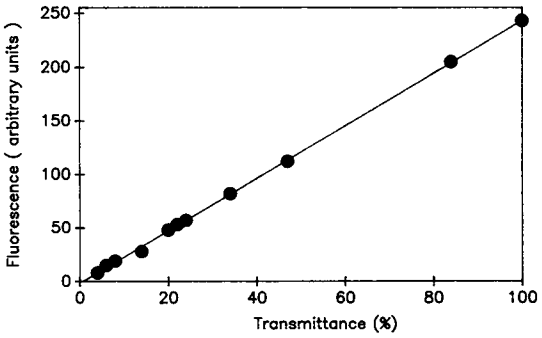

FIGURE 1 Calibration of the SIT camera response. Neutral density optical filters of known transmittance were interposed in the microscope light path to change the excitation light intensity to a predetermined extent. The detected, time-averaged fluorescence intensities from a sample containing 0.2 μM TMRE in EBSS were quantitated by use of the image processor, after background subtraction.

Confocal microscopy

A model MRC-500 (Bio-Rad Laboratories, Cambridge, MA) confocal imaging system was connected to an Axioskop microscope (Carl Zeiss, Inc., Thornwood, NY) equipped with a 63× N.A. 1.25 objective. The 514-nm line of the system's argon ion laser was chosen for excitation of TMRE via a narrow bandwidth excitation filter and a 540-nm dichroic mirror; a 550-nm barrier filter was placed in the emission path. Black level was adjusted so that a uniform gray level of two (out of 255) was obtained with illumination blocked. The gain was adjusted so that with a 1% transmittance neutral density filter in the excitation path, the brightest region of the cell gave a gray level of 250. Images collected with 10% or 0 attenuation of the laser excitation could then be used to accurately measure intensities from less fluorescent regions. A scan rate of 1 frame/s was chosen and, typically, 10 frames were averaged.

Average intensities over specific regions of the cell were measured using the STATS function of the MRC-500 software.

RESULTS

TMRM and TMRE: stable, nontoxic, reversible fluorescent redistribution probes

The distribution of TMRM and TMRE between the extracellular medium, the cell interior, and the intramitochondrial space was very similar both quantitatively and kinetically (for further quantitative comparisons, see Ehrenberg et al., 1988). In the following we will concentrate on results obtained with TMRE. The brightness of the dye fluorescence and the efficiency and sensitivity of the optical system was sufficiently high, so that a 100-W tungsten halogen lamp operating at 40 W could suffice as the excitation source on the microscope for all the dye concentrations employed. This, together with the computer-controlled shutter, obviated the problems of dye bleaching (see Benson et al., 1985) or photodymamic damage to the cells.

The time needed to reach the equilibrium distribution is slower the higher the dye concentration (in the range we explored, 0.1–5.0 μM). Therefore, low concentrations (0.1 or 0.2 μM) were chosen for most experiments, especially because the likelihood of specific and nonspecific damage to the cells increases significantly at higher dye concentrations (see also Discussion). More importantly, equilibration times and final concentrations (as reflected by fluorescence readings) depended on temperature and on the cell line used. All events were significantly sped up at 37°C vs, 22°C and in J774.2 cells as compared to HeLa. To give a few examples, the half-times for reaching the equilibrium distribution of 0.1 μM TMRE were ~6 min at 22°C and 4 min at 37°C for HeLa cells and up to four times faster for J774.2 cells. For comparison, the same half-times for rhodamine 123 in HeLa cells were ~21 min, at 22°C. TMRE penetration into cells can be accelerated up to twofold by the presence of equimolar concentrations of negatively charged tetraphenylborate (TPB) (see Fig. 2), but higher concentrations of TPB seem to have deleterious effects. (It should be noted that the data we chose to present in Fig. 2 are the results for the slowest set of conditions: HeLa cells at 22°C; this made it easier to quantitate the TPB effect). Because the mechanism by which this anion acts on dye distribution could be a complicated one (significant modification of cell surface charges and even direct interaction with the dye are distinct possibilities [Yaginuma et al., 1973]), we did not use TPB in subsequent experiments in spite of the kinetic advantages.

The low membrane binding of both TMRM and

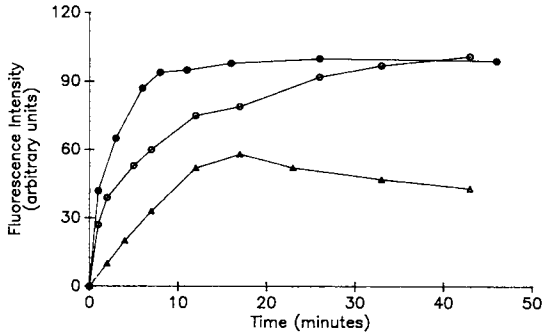

FIGURE 2 Kinetics of dye equilibration and the influence of TPB. The mean intensity of fluorescence from a chosen, fixed area of interest within a HeLa cell was measured with the aid of the image processor for 0.1 μM TMRE equilibration at room temperature (22°C, *open circles*). Addition of equimolar (0.1 μM) TPB accelerated the dye influx (*solid circles*), whereas 2 μM TPB (*triangles*) decreased the detected fluorescence significantly.

TMRE and the reversibility of Nernstian distribution is underscored by the result of successive washes of dye-containing cells with dye-free EBSS: cell fluorescence cannot be distinguished from that of the background (not shown, but see the last panels of Fig. 7, *A* and *B*, for comparison). Upon reexposure to the same dye concentration, the fluorescence of the various regions returns almost exactly to its previous value. By contrast, neither rhodamine 6G nor rhodamine 123 could be fully washed away from the cells, under the same conditions.

The homogeneity and reproducibility of the fluorescence data is illustrated by the following experiment. Upon analysing the cytoplasmic fluorescence intensities of 23 HeLa cells on a coverslip equilibrated with 0.1 μM TMRE in EBSS, we obtained an average value of 82.55 ± 7.32. Under the same experimental conditions, a set of 16 cells from another coverslip, "stained" on a different day, yielded 81.70 ± 8.07. Similar results were obtained for the mitochondrial regions.

Trypan blue exclusion tests, carried out as described in Materials and Methods on cells equilibrated with TMRM and TMRE, revealed a near-complete insensitivity of cell viability to the presence of the dyes. For 0.5 μM TMRE and exposure times of up to 200 min, the viability of HeLa cells was 93% and that of J774.2 cells 96% of the dye-free controls; for the standard concentration used (0.1 μM TMRE) the values were even higher (95 and 99%, respectively).

The ATP concentrations in living cells are remarkably similar, and constitute a good indicator of metabolic competence (Lundin et al., 1986). We used the very sensitive luciferin–luciferase coupled assay to measure the effect of dye exposure on cellular ATP content. The results are summarized in Fig. 3. For an incubation time

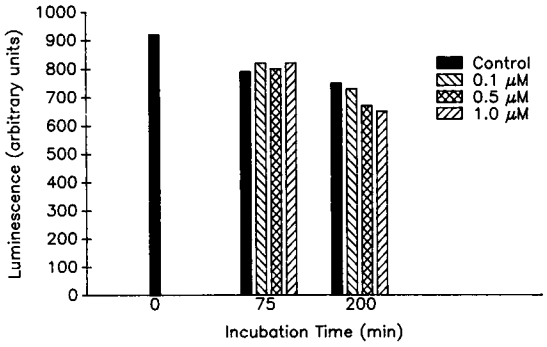

FIGURE 3 ATP content as a measure of cell metabolism: influence of dye addition. ATP was determined by the luciferin–luciferase coupled assay, as described in Materials and Methods. The ordinate is in arbitrary luminescence units, with 1,000 corresponding to 44.5 μg ATP (or 4.5 ± 0.2 pg/cell).

of 75 min, ATP levels were practically unchanged by the presence of TMRE, even at 1.0 μM. After 200 min, some changes start occuring, but for 0.1 μM the concentrations are still (within experimental error) the same as those in the control.

Microscopic observations (in phase contrast) confirm this lack of dye toxicity. For reference, even shorter exposures to certain chemicals (see below) induce not only membrane potential changes but also noticeable structural damage (shape change, blebbing, swelling).

Electron microscopy (Fig. 4) reveals that a 1-h exposure of cells to TMRE (at 37°C) induces no structural changes in the mitochondria, in spite of the rather high local dye concentrations in these organelles as a result of Nernstian accumulation.

The appearance of the cell fluorescence after dye equilibration is illustrated in the early panels of Figs. 5–10. The mitochondrial fluorescence is very pronounced and somewhat punctate in both HeLa and J774.2 cells. Individual mitochondria are not resolvable, however. This has to do not only with mitochondrial size and distribution, but presumably also with rounded shape of these cells. The microscope images fluorescence from a narrow slice centered on the focal plane; with our high numerical aperture objectives the effective width of this slice is ~4 μm. Rounded cells such as the ones used in this study, will display a more diffuse mitochondrial fluorescence because of the contribution from regions of cytoplasm or out of focus mitochondria within this slice. There is

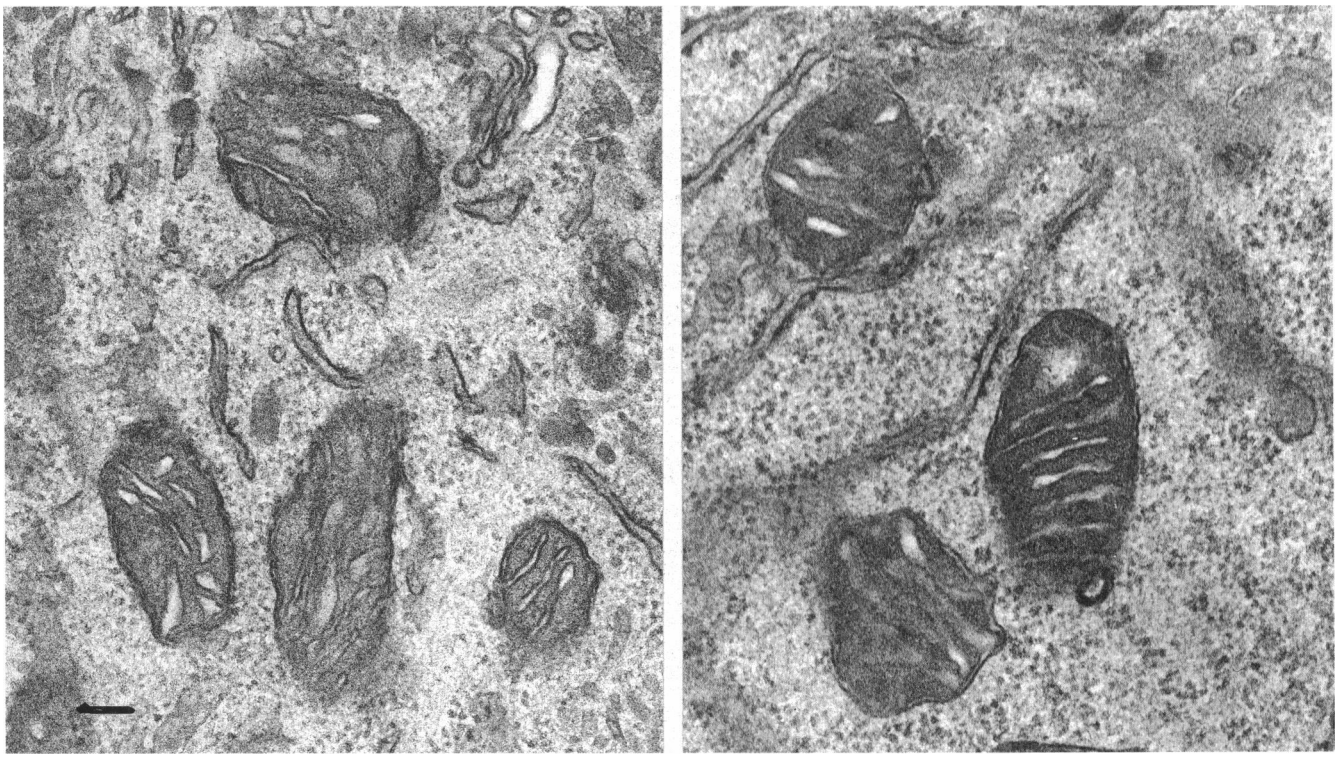

FIGURE 4 Electron microscopy of intracellular structures. Thin-section transmission electron microscopy (see Materials and Methods) reveals no differences in mitochondrial structure between melanoma cells equilibrated in the absence (*left*) or presence of 0.5 μM TMRE (*right*) for 1 h at 37°C. Scale bar in left panel corresponds to 0.2 μm.

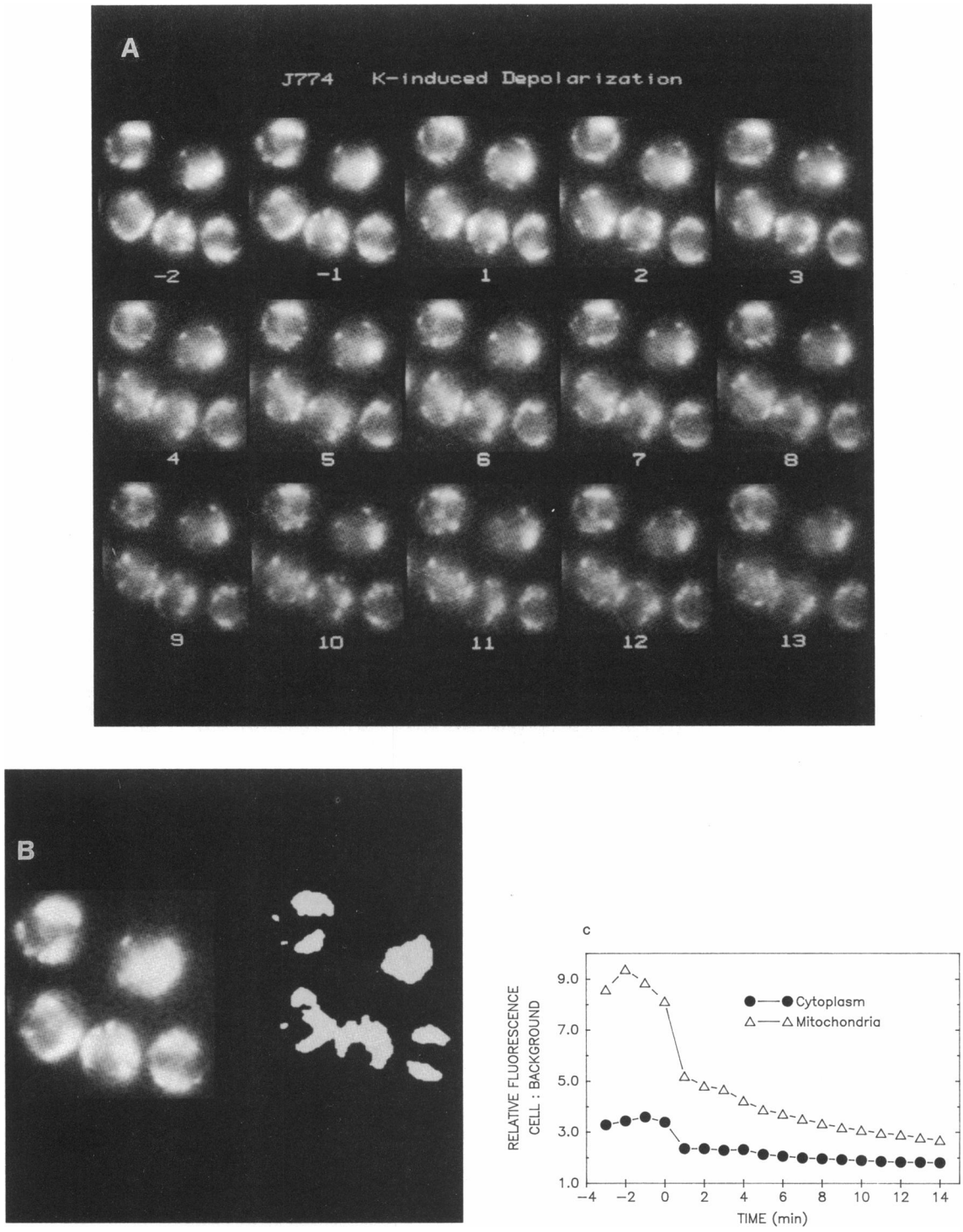

FIGURE 5 Influence of increased potassium concentration on dye fluorescence within J774.2 cells. Exchange of EBSS for KEBSS at time $t = 0$, reduces TMRE (0.1 μM) fluorescence intensity from both mitochondria and cytoplasm. (*A*) Fluorescence images. Time elapsed: 1 min/image. 36°C. Binary templates were created for the mitochondria-rich and mitochondria-free regions of the cells from one prevalinomycin image. The templates were produced by interactively setting high- and low-intensity thresholds to highlight the region of interest. (*B*) The template corresponding to the mitochondria is shown to the right of the image from which it was generated ($t = -1$ min). Each of the sequential images were positioned under this template, as well as the complementary one for the mitochondria-free regions, and the average fluorescence for the respective regions obtained. Data plotted in *C* are these average fluorescence values normalized to the extracellular fluorescence in each frame.

typically a region near the center of the cell which has a lower more uniform fluorescence which can be identified via phase contrast as the nucleus. Because the mitochondria are excluded, and the large nuclear membrane pores place it in electrical equipotential with the cytosol, the nucleus is a convenient region from which to define the mitochondria-free cytoplasmic fluorescence (cf. Ehrenberg et al, 1988).

Selective plasmas membrane depolarization

The membrane potential of adherent J774.2 cells is set primarily by the K^+ distribution (Ehrenberg et al., 1988); therefore, as expected, exposure to the high-potassium buffer reduces overall cell fluorescence, while the mitochondria retain their distinctive punctate pattern (Fig. 5). The decrease in the absolute values of fluorescence in mitochondria is due to the drop in the dye concentrations they are exposed to, as dye equilibration progresses across the depolarized plasma membrane. The analysis in Fig. 5 *C* quantitates this by showing that the mitochondrial fluorescence remains above that of the cytoplasm.

Similarly, the well-characterized, rather nonselective cation channel gramicidin induces a parallel decrease of mitochondrial and cell fluorescence (Fig. 6). The binding of gramicidin to membranes is quite strong, and its equilibration, once bound, has been shown to be rather slow (Clement and Gould, 1981; Loew et al., 1985), i.e., the dissociation of gramicidin from a membrane is slow. Therefore, because the gramicidin molecules must come off the plasma membrane and traverse the outer before they can bind to the inner mitochondrial membrane, depolarization of mitochondria lags far behind and is not

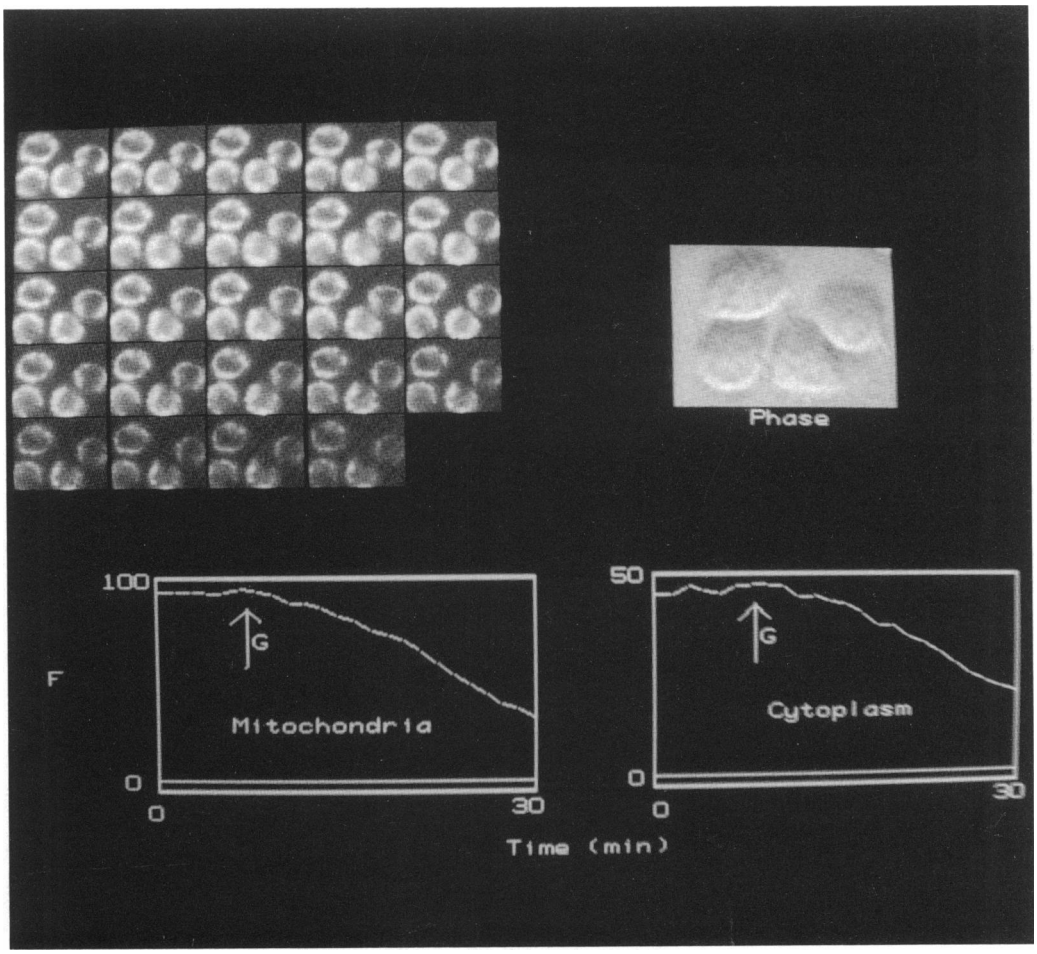

FIGURE 6 Effect of gramicidin on dye fluorescence in cells. Gramicidin (1 μM) was added to HeLa cells preequilibrated with 0.1 μM TMRE in EBSS at 36°C after frame 5 in the sequence shown in upper left. The first 17 images were obtained at 1-min intervals and the rest at 2-min intervals. Templates were created for a pregramicidin image as in Fig. 5, and plots of the total (unnormalized) fluorescence in the mitochondrial and cytoplasmic regions are shown at the bottom.

evident in Fig. 6. As in Fig. 5, the drop in mitochondrial fluorescence can be attributed to the drop in the concentration of dye bathing them. It is also interesting to note that the effect of 1 μM gramicidin is slow (cf. Seligman and Gallin, 1983) compared to the effect of high potassium (Fig. 5). This may be attributed to a slow binding rate, but more likely reflects the cells' ability to combat membrane injuries via ion pumps, recycling, etc.

Effect of valinomycin

The potassium-specific carrier ionophore valinomycin has been extensively used in cell biology to clamp the plasma membrane potential at the potassium ion equilibrium potential. Its effect at 37°C on the cells in our studies is illustrated in Fig. 7. As expected, upon addition of valinomycin and KEBSS to HeLa cells (Fig. 7 *A*), dye fluorescence in both the mitochondrial and cytoplasmic regions decreases rapidly, reflecting the efflux due to the cancellation of both membrane potentials by the ionophore-mediated K movement. Kinetically, the cytoplasmic fluorescence shows a transient increase, as the dye exiting the mitochondria first spills into this volume, exiting the cell soon thereafter; note also the temporary rise (*8'* and *9'*) in extracellular fluorescence as the dye comes spilling out. The end result is reduction of cell fluorescence to the background level within a few minutes. In J774.2 cells (Fig. 7 *B*) similar changes occur, but even faster: within 2 min there is no detectable fluorescence left. At room temperature (22°C) the same sequence of events (data not shown) takes significantly longer, in accordance with the membrane diffusion mechanism of valinomycin action or dye diffusion.

When valinomycin is added to the cells in the presence of a normal external potassium concentration (EBSS), the mitochondrial fluorescence again decreases rapidly with the distinctive punctate pattern blurring away (Fig. 7 *C*), but high levels of cytoplasmic fluorescence

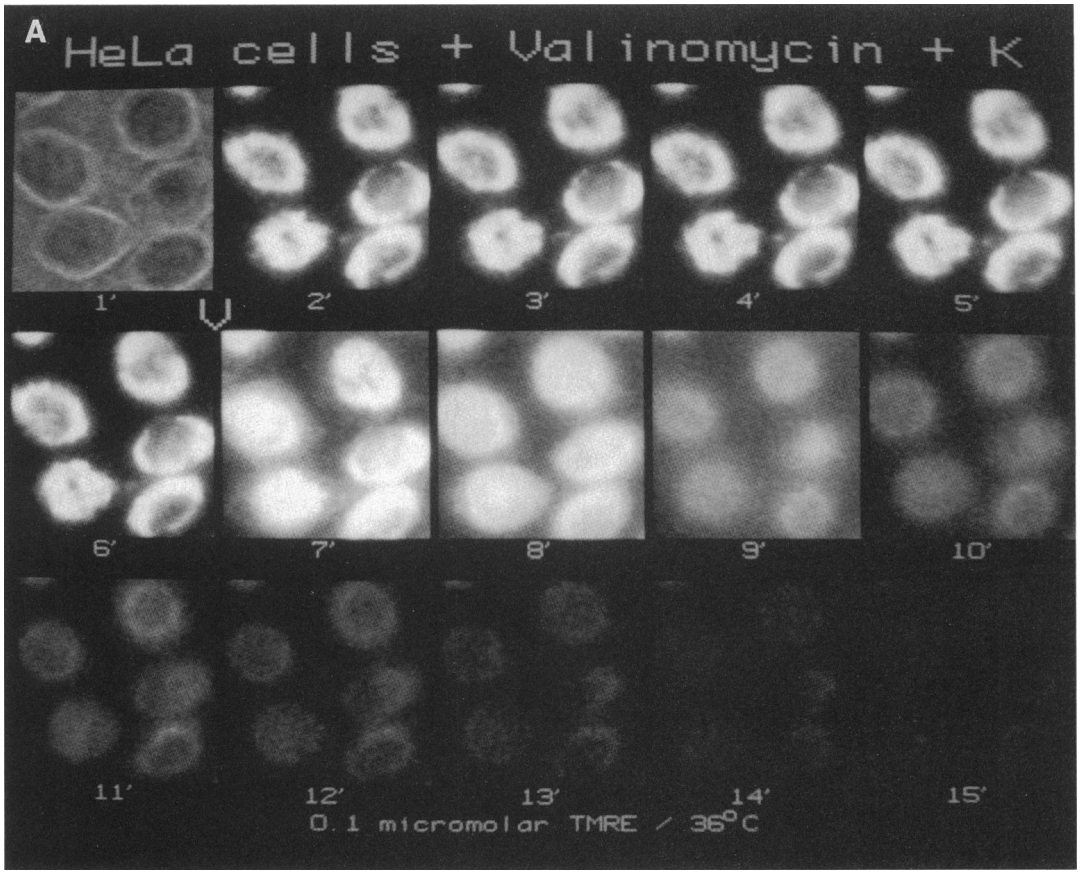

FIGURE 7 Effect of valinomycin on TMRE fluorescence in cells. (*A*) HeLa cells, incubated with 0.1 μM TMRE in EBSS for 20 min at 36°C, with 0.1 μM valinomycin in KEBSS added where indicated (*V*). The first image is phase contrast; the subsequent five are of the cells equilibrated with the dye. Upon valinomycin + KEBSS addition TMRE efflux from mitochondria to the cell interior and from there to the medium occur, as evidenced by the transient fluorescence rise. The extracellular fluorescence eventually decreases to near the original level as the released dye slowly diffuses to the reservoir of the flow chamber.

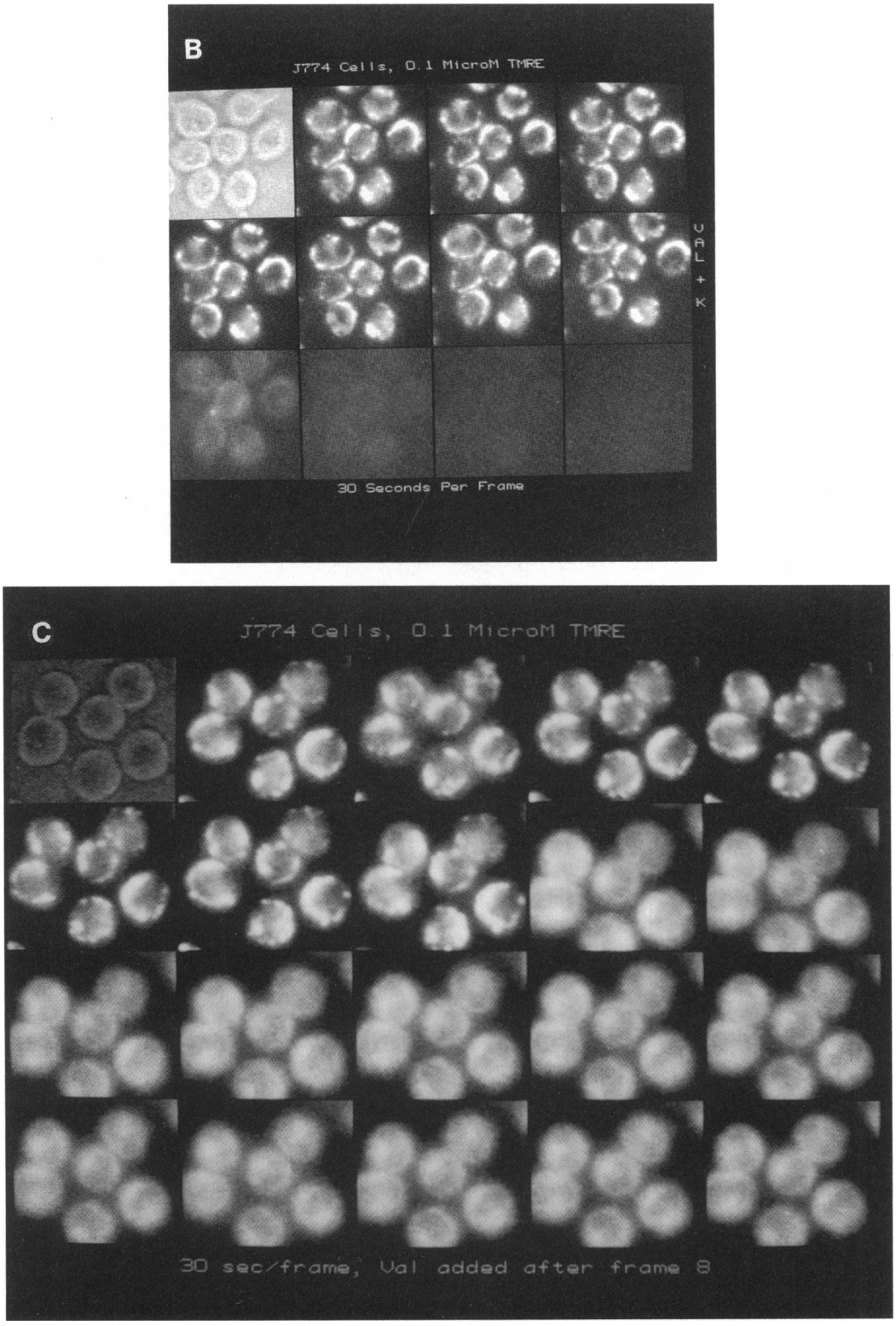

FIGURE 7 (*B*) Same as *A*, for J774.2 cells. Valinomycin and KEBSS are perfused into the chamber between frames 8 and 9 as indicated. Note the significantly faster kinetics of dye efflux (30 s/frame) (extracellular fluorescence eventually falls as in *A* but this data is not shown). (*C*) Same as *B*, but with valinomycin added in normal EBSS (low potassium) between frames 8 and 9. Note the immediate loss of the distinctive punctate mitochondrial fluorescence with no significant cytoplasmic change (on this timescale).

persist. The simplest explanation is that valinomycin again sets the plasma membrane to the K^+ equilibrium potential, but in the absence of added potassium, this is actually slightly hyperpolarizing. After periods longer than that shown in Fig. 7 *C*, a significant decrease does eventually occur, presumably as a result of the metabolic consequences of the ionophore's action.

Effect of FCCP

The best known and most widely used protonophore FCCP is able, by mediating the rheogenic movement of protons, to efficiently collapse the mitochondrial potential in cells (Fig. 8), in a fashion and kinetic pattern similar to valinomycin. Data analysis (Fig. 8 *B*) clearly indicates a pattern of transient rise followed by decrease in the relative cytoplasmic fluorescence; the mitochondrial fluorescence decreases monotonically, and ultimately merges with the cytoplasmic fluorescence. This pattern is quite distinct from that shown in Fig. 5, where only the plasma membrane is depolarized. Combination of FCCP with high K^+ (not shown) leads to a more rapid loss of fluorescence from all regions of the cell, consistent with the proposed mechanism of action.

We investigated a wide range of FCCP concentrations (0.1–10 μM) and although we could discern certain quantitative kinetic differences, we did not find the qualitative distinctions that might be expected between the effects of low and high protonophore concentrations based on a recent report (Reyes and Benos, 1984). At all concentrations, there is a slow depolarization of the plasma membrane which could be attributed to either its depolarization by the protonophore directly, or an indirect effect resulting from depletion of the cell's ATP.

Effect of mitochondrial electron transport inhibitors

The mitochondrial membrane potential is built up in functional organelles by the electron transport associated with oxidative phosphorylation. Several efficient inhibitors of this transport are known and characterized (Singer, 1979), and although the sites and mechanisms of action differ, they should all decrease the mitochondrial membrane potential.

Antimycin A was very effective in doing so, as illustrated in Fig. 9. Mitochondrial dye fluorescence was decreased, with no short-term change in cytoplasmic fluorescence, as expected. Rotenone, another electron transport inhibitor had a similar mode of action, the net result being, however, less pronounced (data not shown). The possible reasons for this quantitative difference are considered in the Discussion.

Effect of energy transfer inhibitors

In mitochondria, the membrane potential is the main component of the electrochemical potential difference which in turn constitutes the driving force for the movement of protons through an ATPase, leading to the synthesis of ATP. If the transfer of energy from the electrochemical potential difference to the functioning of the enzyme is blocked, the net result should be a lesser "load" on the electron transport, and this should lead to an increase in the potential. This has been amply shown for isolated mitochondria, but, to our knowledge, not for mitochondria inside the cell.

Oligomycin is an energy transfer inhibitor of the kind described above, having the ability to block the flow of protons through the membrane-embedded part (F_0) of the ATPase (Linnett and Beechey, 1979). Upon addition to the cells (Fig. 10), it induces the predicted increase in mitochondrial fluorescence. The increase is slow, continuing to develop over a 20-min period. By employing a pseudocolor enhancement, however, the expected increase is evident as early as 2 min after introduction of the drug.

Scanning confocal microscope images of dye distribution

The J774 cells were examined with a confocal laser scanning microscope to see if the resulting images could be used to quantitate membrane potential. It has been shown that a scheme using a photomultiplier positioned over a pinhole measuring diaphragm in the image plane of the microscope, permits the quantitation of fluorescence associated with dye in the cytosol after correction for out of focus contributions (Ehrenberg et al., 1988). The video microscopy scheme employed to obtain Figs. 5–10, on the other hand, can only be used to qualitatively follow changes in fluorescence (i.e., potential). In part, this is due to the limitations of the SIT camera as a light detector (see Discussion), but also derives from the wide apertures in the image plane compared with a microphotometry system. Because confocal microscopy minimizes contributions from out of focus fluorescence by employing extremely narrow apertures in both the image plane and its conjugate plane in the excitation path (White et al., 1987), it was felt that confocal images could be used to measure intracellular fluorescence without a depth of field correction.

A confocal image of a J774 cell stained with TMRE is shown on the left of Fig. 11. The well-defined fluorescence of mitochondria is striking when compared with the images in Figs. 5–10 obtained by conventional fluorescence microscopy. A single mitochondrion is magnified on the right of Fig. 11; this mitochondrion appears to be close

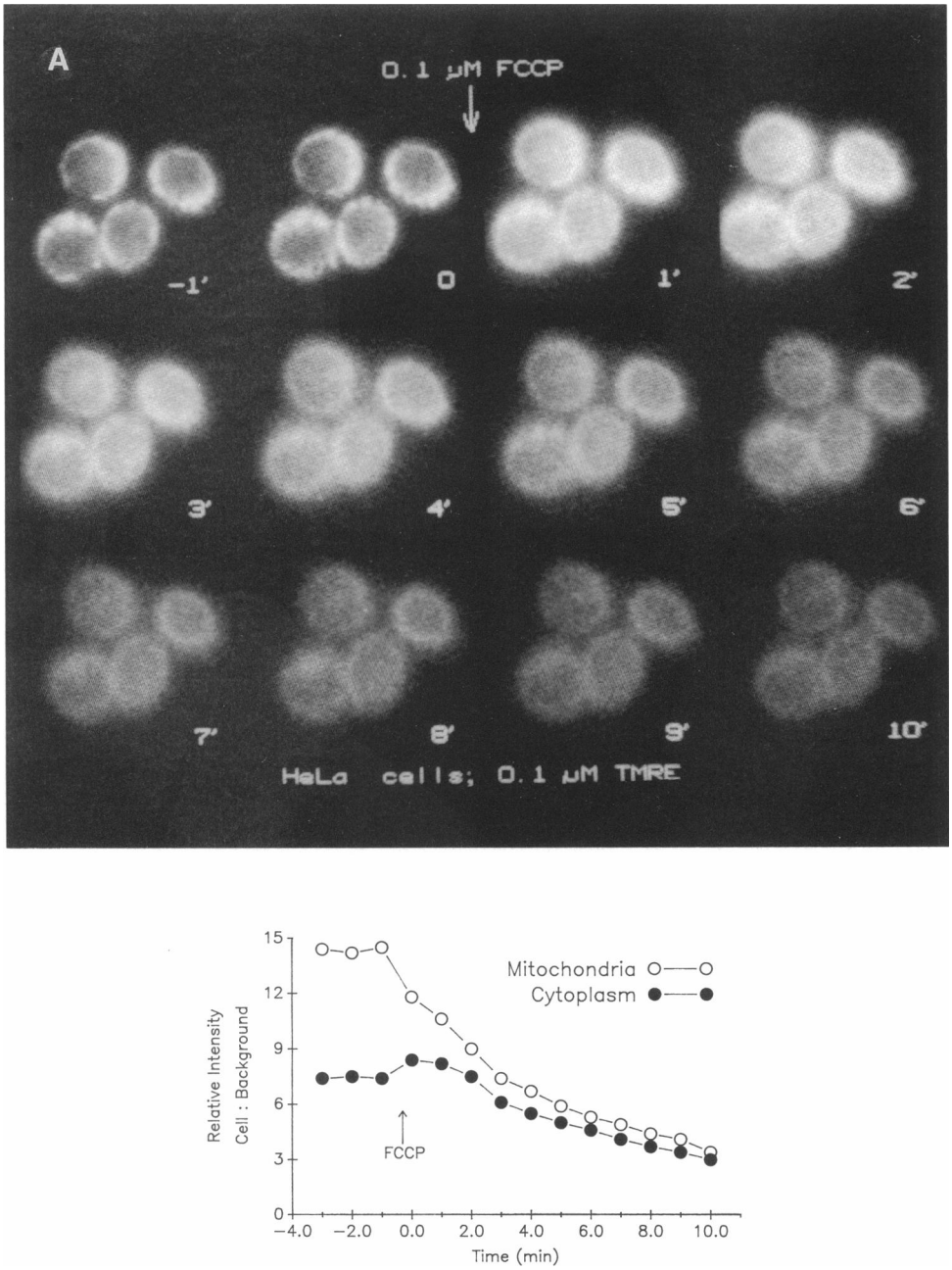

FIGURE 8 Effect of FCCP on dye fluorescence in HeLa cells. FCCP (0.1 μM) was added to cells preequilibrated in 0.1 μM TMRE in EBSS at 36°C. (*A*) Fluorescence images, with elapsed time in minutes; (*B*) analysis of corrected fluorescence intensities in the two regions of interest as in Fig. 5. Fast mitochondrial fluorescence loss is accompanied by a transient increase followed by a slow decrease of cytoplasmic fluorescence.

to the center of the plane of focus and is oriented so its long axis is parallel to the plane. The enlargement helps to accentuate the cristae of the organelle so that they can be visualized. The ratio of intensities from the mitochondrion, the cytosol, and the extracellular medium are 4,700:22:1, respectively. These values were obtained by acquiring separate images with a series of neutral density filters to extend the eight-bit dynamic range of the system electronics. For a cell treated with valinomycin and high potassium (as in Fig. 7 *B*), the corresponding ratios are 15:3:1, indicating the level of nonpotential dependent binding of TMRE. Thus, the potential dependent contributions to the intensity ratios from Fig. 11 are 313:7.4:1 (see Ehrenberg et al., 1988, for a description of this

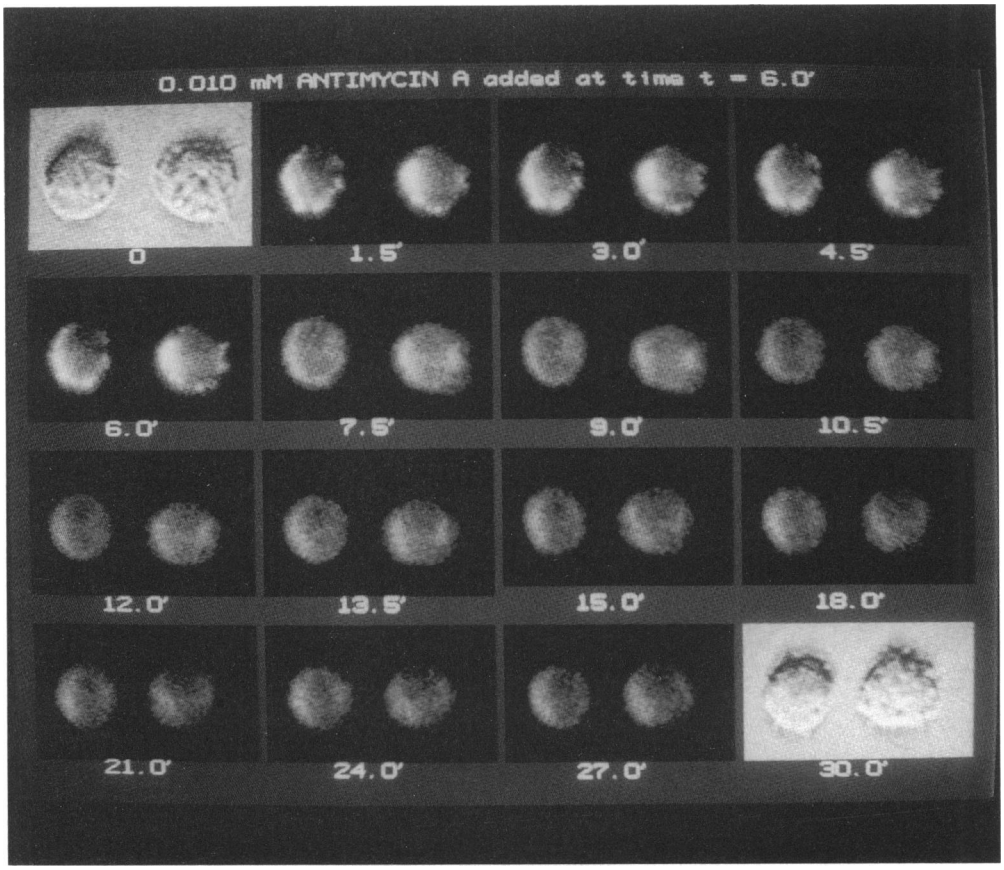

FIGURE 9 Effect of antimycin A on TMRE fluorescence in J774.2 cells. Phase images are shown at $t = 0$ and 30. 10 mM antimycin A was added at time $t = 6$ min in an experimental protocol similar to those in Figs. 5–8. The mitochondrial fluorescence decrease induced was irreversible and, after 30 min, accompanied by swelling and blebbing of the cells, as evidenced by phase-contrast (compare last image to first). Some indication of decay of cytoplasmic fluorescence at later times is consistent with depolarization of the plasma membrane.

analysis). This would translate into potentials of 150 mV and 52 mV for the mitochondrial and plasma membranes, respectively, relative to ground taken extracellularly. This should be considered a lower limit for the mitochondrial potential because not even confocal imaging may be able to extract fluorescence exclusively from a volume as narrow as the mitochondrion.

DISCUSSION

The half-times of dye equilibration we measured were faster than those previously reported for other rhodamine dyes (Johnson et al., 1981; Lampidis et al., 1985). Equilibration of TMRE occurred at least as fast as the fastest nonfluorescent permeant cations (triphenylmethylphosphonium; Hoek et al., 1980). The dependence of dye redistribution kinetics on concentration and temperature was in accordance with expectations, whereas the considerable differences between cell lines were surprising. We also confirmed the acceleration of cationic dye permeation by tetraphenylboron addition, on a timescale significantly faster than that of previous reports (Cheng et al., 1980; Felber and Brand, 1982; Gallo et al., 1984).

The depolarization of both mitochondrial and plasma membrane potentials by valinomycin + KCl was very fast and complete. The decrease in the cells' potential induced by increasing KCl concentrations was equally predictable and in agreement with previous reports (Okada et al., 1973; Ehrenberg, et al; 1988). It should be noted that the addition of KCl to the medium bathing the cells is also expected to induce osmotic swelling, but on a much slower timescale (Jakobsson, 1980). Similarly, the rapid depolarization of mitochondria by both valinomycin and FCCP continues with a subsequent very slow depolarization of the plasma membrane, in all likelihood chiefly the consequence of a secondary depletion of the cells' energy reserves. As a rule, the possibility of the chemical pertur-

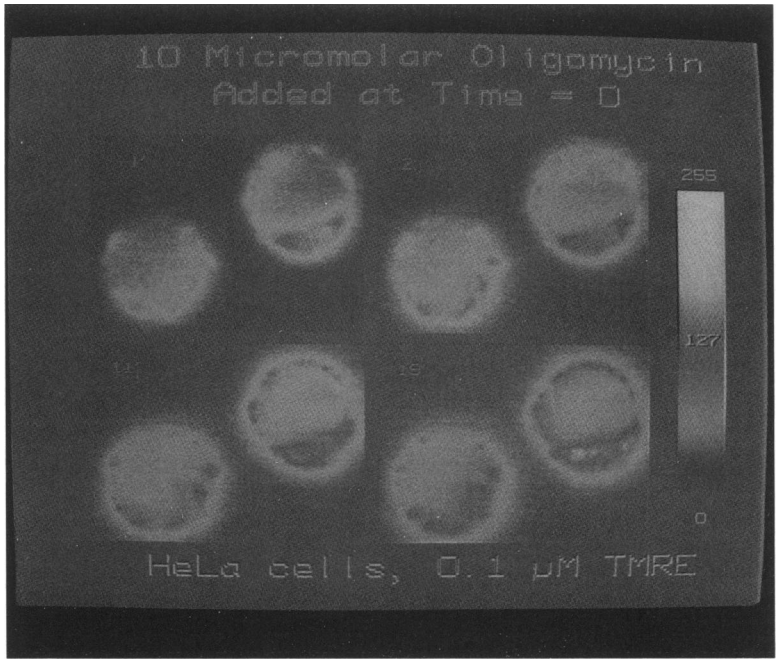

FIGURE 10 Effect of oligomycin on dye fluorescence in cells. HeLa cells incubated in 0.1 μM TMRE in EBSS at 22°C were exposed to 10 μM oligomycin at time $t = 0$. The fluorescence intensities are represented in pseudocolor, with the color scheme shown in the insert. The images correspond to $t = -1$, 2, 11, and 19 min. The regions turning from yellow to red after oligomycin addition correspond to the mitochondrial areas.

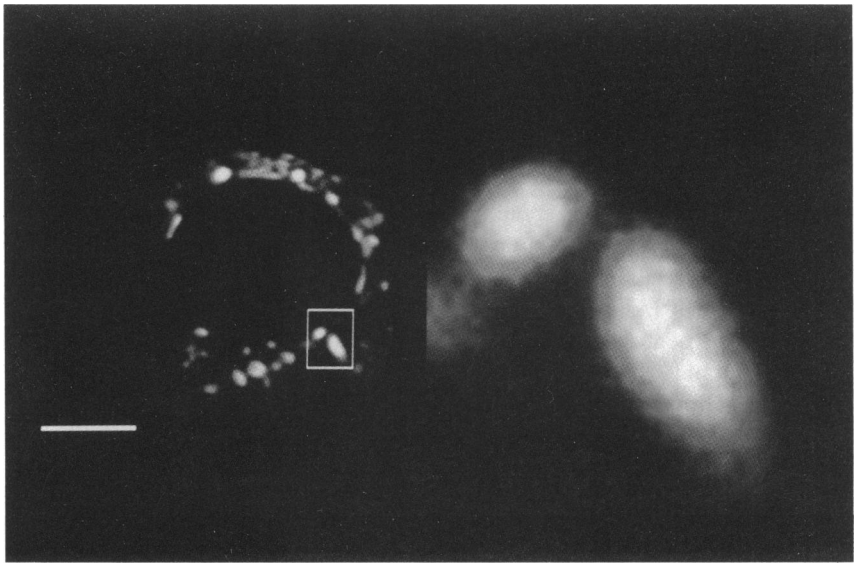

FIGURE 11 Confocal fluorescence image of J774.2 cell. A coverslip containing the cells and equilibrated with 0.1 μM TMRE in EBSS at 37°C was sealed onto a glass slide with paraffin. The slide was mounted on the thermostatted stage of the microscope. An image of a cell is shown on the left. The mitochondrion outlined with a rectangle on the left is magnified on the right. Scale bar, 5 μm.

bants also acting on the membrane potentials through their metabolic effects has to be considered for slow changes. It is apparent that the good time resolution of our method can dissect these phenomena.

The very slow and limited mitochondrial depolarization upon addition of gramicidin is most likely due to its sluggish penetration into the cell interior. Fig. 6 shows that fluorescence decreases at the same rate in both the mitochondria and cytoplasmic regions. The distinctive punctate fluorescence of the mitochondria is maintained throughout. This pattern is characteristic of depolarization of the plasma membrane without substantial depolarization of the mitochondria (cf. Fig. 5). The binding of the very hydrophobic gramicidin molecule and the subsequent dimerization to form a functional cation channel are known to be fast processes (Andersen, 1984). But the dissociation of gramicidin from a membrane can be slow (Clement and Gould, 1981; Loew et al; 1985); it is the dissociation from the plasma membrane, which must necessarily precede gramicidin channel insertion into the mitochondrial membrane, that limits the rate of mitochondrial depolarization.

Significant mitochondrial depolarization was induced by the electron transfer inhibitor antimycin A (Fig. 9). The somewhat lesser influence of rotenone, a well-known inhibitor of electron transfer in isolated mitochondria, may have to do with either its different locus of inhibition in the electron transport chain, the long-known time lag of rotenone action (Singer, 1979), or sluggish penetration into the cell interior, as suggested by Bashford et al. (1985). It is worth mentioning that many studies to date (e.g., Bereiter-Hahn et al., 1983) failed to show any effects of these inhibitors on mitochondrial potentials in situ. It is important to have good kinetic resolution in these measurements as well, because the depletion of available ATP could complicate the picture for longer times.

The increase in mitochondrial membrane potential induced by blocking the proton ATPase by oligomycin has only been shown in situ in two previous reports (Scott and Nicholls, 1980; Hoek et al., 1980), and in both cases the effect barely exceeded experimental error. We can detect this mechanistically expected increase rather easily (Fig. 10). Some reports indicate a decrease in membrane potential upon oligomycin addition (Bereiter-Hahn et al., 1983); we feel that this is a reflection of the limitations of these earlier methods.

A discussion of the limitations and merits of the methodology can be facilitated by reviewing some of these earlier approaches. Let us first compare the method to the use of radiolabeled lipophilic cations (Rottenberg, 1979; Ritchie, 1984). The theory behind the use of nonfluorescent, lipophilic ions such as tetraphenyl phosphonium and triphenylmethylphosphonium, is based on the same Nernstian distribution sketched in the Introduction. Implementation for following time courses requires, however, separate successive measurements on cell aliquots, at the expense of time resolution (Nicholls, 1974; Lichtstein et al., 1979; Sung et al., 1985). Probe accumulation in response to changes in mitochondrial potential can be difficult to distinguish from plasma membrane responses, and quantitation of mitochondrial membrane potentials within cells is very difficult (Hoek et al., 1980). Of course, these are also all bulk measurements on cell suspensions and offer a complementary approach which may be more applicable in certain experimental situations than our measurements on individual cells under the microscope.

Cyanine dyes have also been used primarily to monitor membrane potential in cell, organelle, or vesicle suspensions (Waggoner, 1979; Freedman and Laris, 1981, 1988; Smith, 1988). These studies rely on a change in fluorescence intensity induced by a potential-dependent dye association with the cell. In general, there are two possible mechanisms involving either an overall increase or decrease of fluorescence from the suspension. At low dye concentrations, accumulation of the cationic dye results in a fluorescence enhancement because of the increased quantum yield displayed by cyanines when they are bound to the plasma and organelle membranes. At higher concentrations, accumulation of the dye within the cell and its organelles leads to the formation of nonfluorescent dye aggregates. Thus, although the potential dependence of cyanine dye fluorescence can be calibrated for a suspension of cells and can lead to a highly sensitive and versatile assay, the fluorescence measured from individual cells can have a very complex dependence on potential. Again, the problem of dissecting the contribution of the plasma membrane potential from that of the mitochondria is not easily solved. Still, there have been some reports of successful applications of cyanine dyes to monitor potential in individual cells (e.g., Cohen et al., 1981), and a recent paper uses a cyanine dye to visualize mitochondria via digital imaging microscopy (DeBiasio, et al., 1987).

Of the vast array of other dyes used in studies of cells and intracellular organelles, rhodamines stand out as some of the most extensively employed and investigated, mainly due to their exceptional fluorescence properties. The possible harmful effects of these dyes on cells and cellular components have long been recognized (Gear, 1974; Higuit et al., 1980), and have more recently been studied in great mechanistic detail (Higuti et al., 1980; Mai and Allison, 1983; Wiecker et al., 1987); these effects occur at dye concentrations at least an order of magnitude higher than the ones employed in this study.

Rhodamine 123 is probably the most frequently used dye to visualize mitochondria in living cells (Johnson et al., 1980) and assess their membrane potential (Johnson

et al., 1981; Emaus et al., 1986; Mokhova and Rozovskaia, 1986). Some of the quantitative and mechanistic details in these studies are not fully understood, but it appears that the mechanism by which rhodamine 123 distributes into cells and their mitochondria is, at least in part, the same Nernstian one by which TMRE and TMRM equilibrate. However, it equilibrates much more slowly and is less reversible than TMRE or TMRM (Ehrenberg et al., 1988) making it unsuitable for following the kinetic changes described in this study; its tenacious binding to mitochondria strongly suggests that mechanisms in addition to Nernstian accumulation contribute significantly.

Thus, dye properties, such as membrane permeability, binding, and toxicity, have been improved for the examination of membrane potential in individual cells. Although dye can be quite concentrated in the mitochondria, it has been shown that no significant self-quenching of fluorescence occurs (Ehrenberg et al., 1988). It remains, therefore, to examine the advantages and limitations of the imaging methods employed in this work.

Most of the results of this study were obtained using digital video recording from a conventional fluorescence microscope. Low exciting light levels were possible because of the brightness of the probes and the sensitivity of the SIT camera, obviating problems of photobleaching and photodynamic damage. While timecourses could be monitored conveniently and, using feature extraction algorithms, simultaneously for plasma and mitochondrial membrane potential changes, the amplitudes of the potentials could not be quantitated. There are two reasons for this limitation. First, the camera has a limited dynamic range so that it becomes impossible to measure fluorescence accurately from mitochondria, cytosol, and the extracellular medium. Typically we chose light intensities and camera gain so that the fluorescence intensities of the mitochondria were close to the maximum value of 255, set by the eight-bit resolution of the digitizer. (The effective intrascene dynamic range of the SIT camera is actually only ~80). Some of this dynamic range restriction could be overcome by varying the camera gain in a calibrated way (e.g., by use of neutral density filters) but blooming artifacts from the brighter regions of the cell can then become severe. The second problem has to do with the broad depth of focus associated with conventional microscope optics. The wide field and measuring apertures make it impossible to image individual mitochondria, let alone extract an accurate fluorescence intensity, in the relatively thick rounded cells used in this study (chosen to permit detection of cytosolic fluorescence). Because of these difficulties, we limited ourselves, here, to following the changes induced by membrane-active agents qualitatively. By defining regions enriched in or devoid of mitochondria, we were able to establish various patterns of fluorescence changes which were characteristic of a variety of mechanisms and sites of action.

On the other hand, we felt it important to show that there is no limitation intrinsic to the dyes which precludes quantitation of membrane potential even from regions as small as individual mitochondria. The experiment with the laser scanning confocal microscope demonstrates this. The high degree of resolution along the optical axis permits imaging of individual mitochondria without significant contributions from mitochondria directly above or below the plane of focus. In Fig. 11, the fluorescence from a mitochondrion judged to be bisected by the focal plane was quantitated and compared with intensities obtained from cytosolic and extracellular regions in the image. The latter were obtained by successive removal of neutral density filters; since the image is reconstructed from serially scanned independent photometric measurements, blooming artifacts are absent even when the mitochondrial regions severely saturate the detector. Thus both of the limitations associated with quantitative digital video imaging—restricted dynamic range and broad depth of field—are ameliorated with confocal microscopy (see White et al., 1987, and references cited therein, for reviews of the theoretical and practical aspects of confocal microscopy). The value of 150 mV obtained for the mitochondrial membrane potential seems reasonable but we are unaware of an earlier experimental measurement of mitochondrial potential in situ with which it may be compared. Clearly, the depth of focus, while narrow, is finite, and it is likely that the intensity measured for the mitochondrion is contaminated by some indeterminate volume surrounding it; the value of 150 mV may be, therefore, an underestimate. It should be possible to correct even this presumed error by obtaining optical sections via systematic focusing through the cell. 3-D image reconstruction algorithms (Agard, 1984) can then be applied to these images to obtain corrected fluorescence intensities for the entire ensemble of mitochondria in the cell. On the other hand, the technical difficulties associated with dye bleaching by the highly focused laser should not be underestimated. These would make the acquisition of serial sections quite difficult and totally preclude the use of laser scanning confocal microscopy for the kinds of kinetic monitoring shown in Figs 5–10. Thus, confocal microscopy, at least at its current stage of development, cannot replace conventional microscopy for monitoring the time course of potential changes with these dyes. It does, however, nicely complement the digital video techniques by providing more quantitative measurements of membrane potential at single time points.

We are pleased to acknowledge the assistance of Dr. Dennis Koppel in the development of the imaging software. Dr. Richard Berlin and Dr.

Susan Preston kindly provided the Cloudman melanoma cells and also offered many useful comments on the manuscript. We also thank Chris Pearson for obtaining the electron micrographs.

Support from the United States Public Health Service under grants AI22106 and GM35063 is gratefully acknowledged.

Received for publication 7 February 1989 and in final form 1 August 1989.

REFERENCES

Agard, D. A. 1984. Optical sectioning microscopy: cellular architecture in three dimensions. *Annu. Rev. Biophys. Bioeng.* 13:191–219.

Andersen, O. A. 1984. Gramicidin channels. *Annu. Rev. Physiol.* 46:531–548.

Barrows, G. H., J. E. Sisken, J. C. Allegra, and S. D. Grasch. 1984. Measurement of fluorescence using digital integration of video images. *J. Histochem. Cytochem.* 32:741–746.

Bashford, C. L., G. M. Alder, M. A. Gray, K. J. Micklem, C. C. Taylor, P. J. Turek, and C. A. Pasternak. 1985. Oxonol dyes as monitors of membrane potential: the effect of viruses and toxins on plasma membrane potential of animal cells in monolayer culture and in suspension. *J. Cell. Physiol.* 123:326–336.

Benson, D. M., J. Bryan, A. L. Plant, A. M. Gotto, Jr., and L. C. Smith. 1985. Digital imaging fluorescence microscopy: spatial heterogeneity of photobleaching rate constants in individual cells. *J. Cell Biol.* 100:1309–1323.

Bereiter-Hahn, J., K.-H. Seipel, M. Voth, and J. S. Ploem. 1983. Fluorimetry of mitochondria in cells vitally stained with DASPMI or Rhodamine 6GO. *Cell Biochem. Funct.* 1:147–155.

Berg, H. C., and S. M. Block. 1984. A miniature flow cell designed for exchange of media under high-power microscope objectives. *J. Gen. Microbiol.* 130:2915–2920.

Cheng, K., H. C. Haspel, M. L. Vallano, B. Osotimehin, and M. Sonenberg. 1980. Measurement of membrane potentials of erythrocytes and white adipocytes by the accumulation of triphenylmethylphosphonium cation. *J. Membr. Biol.* 56:191–201.

Clement, N. R., and J. M. Gould. 1981. Kinetics for development of gramicidin-induced ion permeability in unilamellar phospholipid vesicles. *Biochemistry.* 20:1544–1548.

Cohen, L. B., and B. M. Salzberg. 1978. Optical measurement of membrane potential. *Rev. Physiol. Biochem. Pharmacol.* 83:35–88.

Cohen, R. L., K. A. Muirhead, J. E. Gill, A. S. Waggoner, and P. K. Horan. 1981. A cyanine dye distinguishes between cycling and non-cycling fibroblasts. *Nature (Lond.).* 290:593–595.

Debiasio, R., G. R. Bright, L. A. Ernst, A. S. Waggoner, and D. L. Taylor. 1987. Five parameter fluorescence imaging: wound healing of living Swiss 3T3 cells. *J. Cell Biol.* 105:1613–1622.

Ehrenberg, B., V. Montana, M.-D. Wei, J. P. Wuskell, and L. M. Loew. 1988. Membrane potential can be determined in individual cells from the Nernstian distribution of cationic dyes. *Biophys. J.* 53:785–794.

Emaus, R. K., R. Grunwald, and J. J. Lemasters. 1986. Rhodamine 123 as a probe of transmembrane potential in isolated rat-liver mitochondria: spectral and metabolic properties. *Biochim. Biophys. Acta.* 850:436–448.

Felber, S. M., and M. D. Brand. 1982. Factors determining the plasma-membrane potential of lymphocytes. *Biochem. J.* 204:577–585.

Freedman, J. C., and P. C. Laris. 1981. Electrophysiology of cells and organelles: studies with optical potentiometric indicators. *In* Membrane Research: Classic Origins and Current Concepts. A. L. Muggleton-Harris, editor. Academic Press, Inc., New York. 177–246.

Freedman, J. C., and P. C. Laris. 1988. Optical potentiometric indicators for nonexcitable cells. *In* Spectroscopic Membrane Probes. Vol. 3. L. M. Loew, editor. CRC Press, Inc., Boca Raton, FL. 1–49.

Gallo, R. L., J. N. Finkelstein, and R. H. Notter. 1984. Characterization of the plasma and mitochondrial membrane potentials of alveolar type II cells by use of ionic probes. *Biochim. Biophys. Acta.* 771:217–227.

Gear, A. R. L. 1974. Rhodamine 6G: a potent inhibitor of mitochondrial oxidative phosphorylation. *J. Biol. Chem.* 249:3628–3637.

Higuti, T., S. Niimi, R. Saito, S. Nakasima, T. Ohe, I. Tani, and T. Yoshimura. 1980. Rhodamine 6G, inhibitor of both H^+ ejections from mitochondria energized with ATP and with respiratory substrates. *Biochim. Biophys. Acta.* 593:463–467.

Hoek, J. B., D. J. Nicholls, and J. R. Williamson. 1980. Determination of the mitochondrial protonmotive force in isolated hepatocytes. *J. Biol. Chem.* 255:1458–1464.

Jakobsson, E. 1980. Interactions of cell volume, membrane potential, and membrane transport parameters. *Am. J. Physiol.* 238:C196–C206.

Johnson, L. V., M. L. Walsh, and L. B. Chen. 1980. Localization of mitochondria in living cells by rhodamine 123. *Proc. Natl. Acad. Sci. USA.* 77:990–994.

Johnson, L. V., M. L. Walsh, B. J. Bockus, and L. B. Chen. 1981. Monitoring of relative mitochondrial membrane potential in living cells by fluorescence microscopy. *J. Cell Biol.* 88:526–535.

Kochan, S. G. 1983. Programming in "C." Hayden Book Co., Hasbrouck Heights, NJ.

Korchak, H. M., A. M. Rich, C. Wilkenfeld, L. E. Rutherford, and G. Weissmann. 1982. A carbocyanine dye, $DiOC_6(3)$, acts as a mitochondrial probe in human neutrophils. *Biochem. Biophys. Res. Commun.* 108:1495–1501.

Lampidis, T. J., Y. Hasin, M. J. Weiss, and L. B. Chen. 1985. Selective killing of carcinoma cells in vitro by lipophilic-cationic compounds: a cellular basis. *Biomed. Pharmacother.* 39:220–226.

Leach, F. J., and J. J. Webster. 1986. Commercially available firefly luciferase reagents. *Methods Enzymol.* 133:51–70.

Lichtstein, D., H. R. Kaback, and A. J. Blume. 1979. Use of a lipophilic cation for determination of membrane potential in neuroblastoma: glioma hybrid cell suspensions. *Proc. Natl. Acad. Sci. USA.* 76:650–654.

Linnett, P. E., and R. B. Beechey. 1979. Inhibitors of the ATP synthetase system. *Methods Enzymol.* 55:472–518.

Loew, L. M. 1988. Spectroscopic Membrane Probes. CRC Press, Inc., Boca Raton, FL. Chapters 14–21.

Loew, L. M., L. Benson, P. Lazarovici, and I. Rosenberg. 1985. Fluorometric analysis of transferable membrane pores. *Biochemistry.* 24:2101–2104.

Lundin, A., M. Hasenson, J. Persson, and A. Pousette. 1986. Estimation of biomass in growing cell lines by adenosine triphosphate assay. *Methods Enzymol.* 133:27–42.

Mai, M. S., and W. S. Allison. 1983. Inhibition of an oligomycin-sensitive ATPase by cationic dyes, some of which are atypical uncouplers of intact mitochondria. *Arch. Biochem. Biophys.* 221:467–476.

Mokhova, E. N., and I. A. Rozovskaya. 1986. The effects of mitochondrial energetics inhibitors on the fluorescence of potential-sensitive

dyes Rhodamine 123 and DiS-C_3(5) in lymphocyte suspensions. *J. Bioenerg. Biomembr.* 18:265–276.

Nicholls, D. G. 1974. The influence of respiration and ATP hydrolysis on the proton-electrochemical gradient across the inner membrane of rat-liver mitochondria as determined by ion distribution. *Eur. J. Biochem.* 50:305–315.

Okada, Y., M. Ogawa, N. Aoki, and K. Izutsu. 1973. The effect of K on the membrane potential of HeLa cells. *Biochim. Biophys. Acta.* 291:116–126.

Paul, J. 1970. Cell and Tissue Culture. 4th ed. E. & S. Livingstone, Ltd., Edinburgh, UK

Preston, S. F., M. Volpi, C. M. Pearson, and R. D. Berlin. 1987. Regulation of cell shape in the Cloudman melanoma cell line. *Proc. Natl. Acad. Sci. USA.* 84:5247–5251.

Reyes, J., and D. J. Benos. 1984. Changes in interfacial potentials induced by carbonylcyanide phenylhydrazone uncouplers: possible role in inhibition of mitochondrial oxygen consumption and other transport processes. *Membr. Biochem.* 5:243–268.

Ritchie, R. J. 1984. A critical assessment of the use of lipophilic cations as membrane potential probes. *Prog. Biophys. Mol. Biol.* 43:1–32.

Rottenberg, H. 1979. The measurement of membrane potential and pH in cells, organelles, and vesicles. *Methods Enzymol.* 55:547–569.

Scott, I. D., and D. G. Nicholls. 1980. Energy transduction in intact synaptosomes: influence of plasma-membrane depolarization on the respiration and membrane potential of internal mitochondria determined in situ. *Biochem. J.* 186:21–33.

Seligman, B. E., and J. I. Gallin. 1983. Comparison of indirect probes of membrane potential utilized in studies of human neutrophils. *J. Cell. Physiol.* 115:105–115.

Singer, T. P. 1979. Mitochondrial electron-transport inhibitors. *Methods Enzymol.* 55:454–462.

Smith, J. C. 1988. Potential-sensitive molecular probes in energy-transducing organelles. *In* Spectroscopic Membrane Probes. Vol. 2. L. M. Loew, editor. CRC Press, Inc., Boca Raton, FL. 153–197.

Sung, S.-S. J., J. D.-E. Young, A. M. Origlio, J. M. Heiple, H. R. Kaback, and S. C. Silverstein. 1985. Extracellular ATP perturbs transmembrane ion fluxes, elevates cytosolic Ca^{2+}, and inhibits phagocytosis in mouse macrophages. *J. Biol. Chem.* 260:13442–13449.

Waggoner, A. S. 1979. Dye indicators of membrane potential. *Annu. Rev. Biophys. Bioeng. 8:847–868.*

Waggoner, A. S. 1985. Dye probes of cell, organelle, and vesicle membrane potentials. *In* The Enzymes of Biological Membranes. A. N. Martonosi, editor. Plenum Publishing Corp., New York. 313–331.

White, J. G., W. B. Amos, and M. Fordham. 1987. An evaluation of confocal versus conventional imaging of biological structures by fluorescence light microscopy. *J. Cell Biol.* 105:41–48.

Wiecker, H.-J., D. Kuschmitz, and B. Hess. 1987. Inhibition of yeast mitochondrial F_1-ATPase, F_0F_1-ATPase and submitochondrial particles by rhodamines and ethidium bromide. *Biochim. Biophys. Acta.* 892:108–117.

Yaginuma, N., S. Hirose, and Y. Inada. 1973. Spectral change of Rhodamine 6G caused by the energization of mitochondria, in relation to charge separation. *J. Biochem.* 74:811–815.